Validated Open-source Modelica Model of Direct Evaporative Cooler with Minimal Inputs

Saranya Anbarasu ^{1,4}, Wangda Zuo ^{1,2}*, Yangyang Fu ¹, Yash Shukla ³, Rajan Rawal ^{3,4}

¹ Department of Civil, Environmental and Architectural Engineering, University of Colorado Boulder, Boulder, CO, USA

² National Renewable Energy Laboratory, Golden, CO, USA

³ Centre for Advanced Research in Building Science and Energy, CRDF, CEPT University, Ahmedabad, India

⁴ Faculty of Technology, CEPT University, Ahmedabad, India

^{*}Corresponding author: wangda.zuo@colorado.edu

Abstract

Direct evaporative coolers (DECs) are a low-energy cooling alternative to conventional air conditioning in hot-dry climates. The key component of DEC is the cooling pad, which evaporatively cools the air passing through it. While detailed numerical models of heat and mass transfer have been proposed for the cooling pad, these require many input parameters that are not readily accessible. Alternatively, simplified models lack accuracy and are confined to a common type of cooling pad. To address these limitations, we developed and validated a physics-based model for the evaporative cooling pad that only needs the nominal data to compute the heat and mass transfer with considerable accuracy. The proposed model is implemented in Modelica, an equation-based object-oriented modeling language. For comparison, a basic lumped model from EnergyPlus based on the efficiency curve of the cooling pad is also implemented. The physics-based model exhibits <2% error from the experimental data and the lumped model exhibits a 12.3% error.

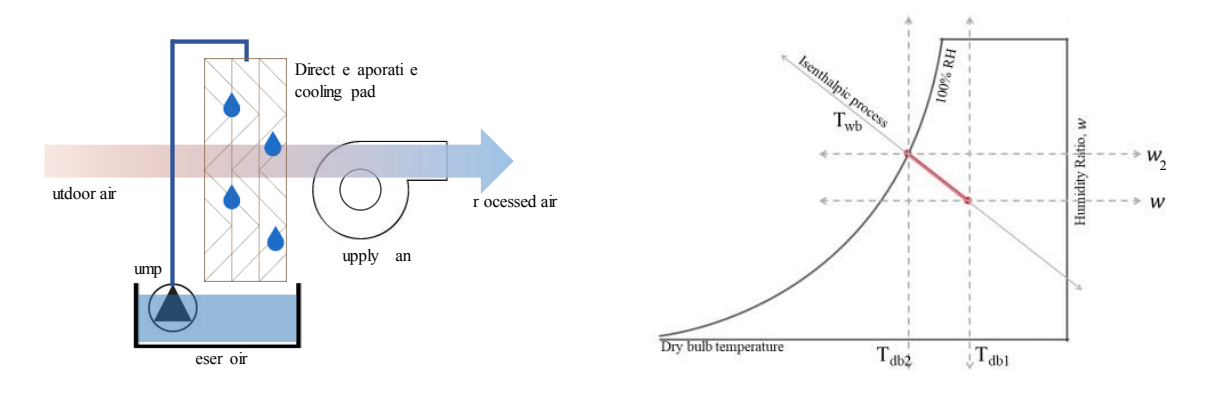
Keywords: Direct evaporative cooler, Modelica, Physics-based model.

1. Introduction

Conventional air conditioners that are based on the vapor compression refrigeration cycle are being used for cooling in residential and commercial buildings throughout the world. These conventional systems employ refrigerants like hydrochlorofluorocarbons (such as R-22) and hydrofluorocarbon (such as R-134a, and R-410A) that have high global warming potential (GWP) (Weubbles, 1994). Despite these systems having high GWP, they are commercially dominant as conventional systems are stable in space conditioning (Vakiloroaya et al., 2014). For regions with hot and dry climates, energy consumption for space cooling is over 60% of the total energy used in buildings (Boukhanouf et al., 2014). To reduce the energy consumption of conventional systems, alternative options such as evaporative cooling can be utilized to significantly save energy and reduce CO₂ emissions (Dodoo, 2011). The evaporative cooling system is more environmentally friendly as it uses water instead of refrigerants as the working fluid to cool the air through the process of evaporation (ASHRAE, 2013). Though direct energy comparisons cannot be made between the DECs (open systems) and conventional closed systems, DECs can be used to augment the energy savings of conventional systems. Over the recent years, there has been extensive research on precooling components that can reduce the peak cooling load of the cooling system. In addition to DECs, there are (1) indirect evaporative coolers (IEC) that lower the temperature without the increase in relative humidity; (2) hybrid coolers that have direct, indirect, and DX coils connected in series; and (3) dew point evaporative coolers that can cool the air below wet bulb temperature to have proven heat recovery and pre-cooling benefits in hot and dry climates (Sajjad et al., 2021). One such experimental testing exhibits a 22.9-35.1% peak cooling load reduction by using DEC and IEC as pre-cooling components for central air-conditioning systems (Chen et al., 2014; Min et al., 2021).

Figure 1 shows a typical Direct Evaporative Cooler (DEC), with the key component being the cooling pad that serves as heat and mass exchangers that are built with layers of humidity-absorbing materials such as cellulose, aspen, paper, etc. The cooling pad is wetted using a pump. A centrifugal fan blows the air through the wetted cooling pad, which cools the dry air by increasing the relative humidity. Thermodynamically, the energy required to evaporate the water is taken from the air in the form of sensible heat and is converted into latent heat. This conversion of sensible heat to latent heat, without the change in enthalpy, is known as an isenthalpic process. Figure 2 represents the direct evaporative cooling process on the psychrometric chart as a parallel

line to the wet bulb line and the enthalpy line. Evaporative cooling, therefore, causes a drop in the air temperature, proportional to the sensible heat drop, and an increase in relative humidity, proportional to the latent heat gain (Fouda & Melikyan, 2011). The extent of temperature drop depends on the duration of contact, the surface area of contact, and the mass flow rate of air passing through the cooling pad. There is also a considerable pressure drop depending on the geometric configuration of the cooling pad, which must be accounted for by the fan to maintain the specific outlet mass flow rate.



cooler with a built-in pump and fan

Figure 1 Diagram of a typical direct evaporative Figure 2 Direct evaporative cooling process on the psychrometric chart

2. Existing Numerical Heat and Mass Transfer Models of DEC

The passive cooling potential of DECs has been established for various climates in past years (Venkateswara Rao & Datta, 2020; Saman et al., 2010; Kowalski & Kwiecień, 2020; Jaber & Ajib, 2011), yet research demands still exist due to the limited technical data and numerical models (Amer et al., 2015). Prior investigations led to diverse approaches to developing numerical models for evaporative coolers (Table 1); however, they are not open source, not flexible, and require to be implemented by the user in the preferred computational tool. In 1980, Holman described a numerical heat and mass transfer method to calculate the performance of evaporative cooling systems based on the E-NTU method of the heat exchanger (Holman, 1980). Maclaine-Cross and Banks (1981) added a linear function of the air saturation line and a stationary water film. By 1987, there was a proposal for a generic correlation of heat and mass transfer coefficients using Nusselt's Nu, and Sherwood number Sh, for rigid cellulose media by Dowdy and Karabash (1987). Several other researchers extended Dowdy's model by proposing Nu and Sh correlations for various evaporative media and configurations using experiments (A. Franco et al., 2010; He et al., 2015).

Dai and Sumathy (2002) proposed an elaborate model with governing equations of liquid film and gas phases, as well as the interface conditions between the media. Kachhwaha and Prabhakar (2010) incorporated the impact of elevated water temperature on the cooling efficiency, by adding dimensionless correlation coefficients (α , ϕ , β). The latest research by Ko a če ić and ourbron (2017) proposed an energy and mass conservation model of humid air and water in a one-dimensional geometry by applying correlations for heat and mass transfer coefficients. Most of these methods can predict the performance of DECs with 85-98% accuracy but require few measured values from experiments to supplement the mathematical model. Using assumptions to parameters such as the temperature of water at the media interface, the number of segments in the cooling pad, enthalpy correction factor, Nu, and Sh, etc., can result in significant variations in the model prediction. Thus, there is a need for a new DEC model, which only requires the basic and easily accessible input information yet provides accurate predictions.

Table 1 Existing research on heat and mass transfer of DECs

Method	Reference	Description of the model	Accuracy	
1	(Holman, 1988)	-		
		and heat balance with the saturation		
		efficiency on the evaporative cooling		
		rigid media.		
2	(Maclaine-Cross	Proposed a linear function regarding the	98%	
	& Banks, 1981)	air saturation line and a stationary water		
		film.		
3	(Kettleborough &	Counterflow evaporative cooler using	-	
	Hsieh, 1983)	the theory of enthalpy potential		
4	(Dowdy et al.,	Correlations to determine the	87%	
	1986;	convective heat and mass transfer		
	Dowdy &	coefficients using Nusselt's number and		
	Karabash, 1987)	chmidt's number		
5	(Halasz, 1998)	Detailed heat and mass transfer with	Theoretical paper	
		partial differential equations		
6	(Camargo &	E-NTU method to compute heat transfer	87%	
	Ebinuma, 2003)	coefficients accounting for the wet		
		surface heat transfer.		
7	(Dai & Sumathy,	The governing equations of liquid film	Outlet temperature	
	2002)	and gas phases, as well as the interface	prediction \pm	
		conditions, have been accounted for.	0.25°C	

8	(Wu et al., 2009)	Introduction of cooling pad geometry and configuration correlations into the	Outlet temperature prediction ±
		efficiency equation.	0.15°C
9	(Kachhwaha &	Dimensionless correlations for ε -NTU,	90%
	Prabhakar, 2010)	accounting for elevated water	
		temperatures.	
10	(Fouda &	A simplified model with heat and mass	Outlet temperature
	Melikyan, 2011)	correlation equations.	prediction ± 0.7 °C
11	(Sodha &	Impact of stratification of water	89%
	Somwanshi,	temperature variation along with the	
	2012)	cooling pad.	
12	(Crawley et al.,	Effectiveness is calculated using a	-
	2001)	curve fit equation specific to the	
		CELdek cooling pad.	
13	(Ko a če ić &	Energy and mass conservation	97%
	Sourbron, 2017)	equations of humid air and water in a	
		one-dimensional geometry by applying	
		correlations for heat and mass transfer	
		coefficient.	

Correspondingly, in the building energy modeling and simulation industry, there are limitations in the availability of validated DEC models in the existing simulation tools. DOE-2 (Winkelmann et al., 1993) and IES (IESVE, 2011) have validated single and two-stage DEC models, where the outlet conditions are based on efficiency (user input value). EnergyPlus contains component models for direct and indirect evaporative coolers based on an industrial standard CelDek cooling pad (Crawley et al., 2001). EnergyPlus also gives a research special component that calculates operation efficiency using an efficiency modifying curve and part load fraction of a static efficiency input. Thus, the EnergyPlus models are only limited to cellulose cooling pads. With advancements in interactive buildings, there arrives a need to dynamically test the performance of systems and components that are non-linear and complex (Trčka et al., 2009). Thus, a flexible simulation method that can satisfy the above needs is desired.

To overcome these issues, this research develops and validates a physics-based DEC model which is (1) capable of accurate heat and mass transfer predictions using the easily available catalog data; (2) flexible enough to be modeled and simulated for various needed, such as an entire DEC system model, cooling pad model, individual blocks that can facilitate alternative

heat and mass transfer equations testing, etc.; (3) an open-source model contribution to support the growing needs of the modeling community (freely available at: https://github.com/sbslab/DirectEvaporativeCooler/tree/jbps)

To cater to these needs, we have implemented the new DEC model in Modelica, which is an equation-based object-oriented modeling approach, capable of testing complex, dynamic, and nonlinear systems (Elmqvist & Mattsson, 1997). Modelica facilitates component-based modeling which is useful to build the heat and mass transfer equations as individual blocks and integrate them as cooling pad components and then as a system. There are many open-source Modelica libraries for building systems such as Modelica Buildings library (MBL), IDEAS, AixLib, Building Systems, etc. that are under constant development (Wetter et al., 2014; Jorissen et al., 2018; Mehrfeld et al., 2016; and Plessis et al., 2014). Models similar to the direct evaporative cooler are not available in the commonly used open-source Modelica libraries, which also substantiates the need for developing this open-source model in Modelica. The rest of this paper is organized as follows: Section 3 introduces two mathematical models for the evaporative cooling pad with a varying degree of input parameters, (i) a lumped model, and (ii) a detailed physicsbased model. Section 4, describes the Modelica implementation of the evaporative cooling pad models and the integrated DEC system model. Section 5, describes the evaluation of the cooling pad with the DEC system by comparing the performance to the experimental data from the literature. At last, simulation results are summarized and concluding remarks of this paper are made.

3. Mathematical Model Description

3.1 Lumped Cooling Pad Model

The lumped cooling pad model is based on the model implemented in the well-known simulation program EnergyPlus (Crawley et al., 2001). The outlet conditions of the lumped model depend primarily on the efficiency of the cooling pad η . The η function used in EnergyPlus is derived based on the manufacturer's data for the saturation efficiency at a rious air e locities and pad thicknesses. The least-squares routine produced an eleven-term multi-variate fit using a third-order quadratic. This equation is limited to the commonly used Munter's CelDek cooling pad. The efficiency equation needs modifications to support various cooling pad media and can be determined only through experiments.

$$\begin{split} \eta &= 0.792714 + 0.958569 \, d - 0.25193 \, v_a - 1.03215 \, d^2 + 0.0262659 \, v_a^2 \\ &\quad + 0.914869 \, (d * v_a) - 1.4821 \, (d^2 * v_a) - 0.018992 \\ &\quad + 1.13137 (d^3 * v_a) + 0.0327622 (d^2 * v_a^3) - 0.145384 (d^3 * v_a^2) \end{split} \label{eq:eta_delta_state} \tag{I}$$

where d is the thickness (m) and v_a is the velocity at the face of the cooling pad $(m \, s^{-1})$. Using the calculated η from eq.(1), the dry bulb temperature of the outlet air can be estimated using the efficiency relationships of evaporative systems:

$$\eta = \frac{T_{db,in} - T_{db,ou}}{T_{db,in} - T_{wb,ou}},$$
(2)

where $T_{db,in}$ and $T_{db,ou}$ are the inlet and outlet dry bulb temperature (°C) and $T_{wb,in}$ is the inlet wet bulb temperature (°C). As evaporative cooling is an isenthalpic process, the inlet wet bulb temperature $T_{wb,in}$ is equal to the outlet wet bulb temperature $T_{wb,ou}$,

$$T_{wb.in} = T_{wb.ou}. (3)$$

Based on this assumption, the resulting humidity ratio of the outlet w_{ou} , is calculated using the psychrometric properties of air described in Appendix. The volume flow rate of water evaporated $\dot{V}_{eva}(m^3s^{-1})$, which is added to the airside is determined using,

$$\dot{V}_{eva} = \frac{\dot{m}_a(w_{ou} - w_{in})}{\rho_w},\tag{4}$$

where \dot{m}_a , is the mass flow rate of air $(kg \ s^{-1})$; w_{ou} and w_{in} are the outlet and inlet humidity ratios $(kg_w kg_a^{-1})$; and ρ_w is the density of water $(kg m^3)$ (standard density of water at 25°C is used). Once the properties of the outlet air are determined, the total volume flow rate of water consumption can be determined using the,

$$\dot{V}_{tot} = \dot{V}_{eva} + \dot{V}_{dri} + \dot{V}_{blo}. \tag{5}$$

$$\dot{V}_{dri} = \dot{V}_{eva} f_{drift}, \tag{6}$$

$$\dot{V}_{dri} = \dot{V}_{eva} f_{drift}, \tag{6}$$

$$\dot{V}_{blo} = \frac{\dot{V}_{evap}}{R_{con} - 1} - \dot{V}_{drift}. \tag{7}$$

where \dot{V}_{tot} is the total volume of water consumed (m^3s^{-1}) ; \dot{V}_{dri} is the volume flow rate of water leaving as droplets on the supply side (m^3s^{-1}) ; \dot{V}_{blo} is the volume flow rate of water drained from the sump to counter the build-up of solids in the water that would otherwise occur because of evaporation (m^3s^{-1}) ; f_{drift} is the drift factor $(f_{drift}=0)$ if the system has no losses); and R_{con} is the ratio of solids in blowdown water compared to freshwater.

3.2 Physics-based Cooling Pad Model

The physics-based cooling pad model is built based on the governing equations of the heat and moisture transfer between water and air. The rate of sensible dq_s , and latent heat transfer dq_l , along a small thickness of the cooling pad dx is defined as,

$$dq_{s} = h_{c} dA \left(T_{dh} - T_{w} \right), \tag{8}$$

$$dq_l = h_m h_{vs} dA (w_s - w_a), (9)$$

where dA is the surface area (m^2) represented as the product of breadth and height $(=bh\,dx)$ of the cooling pad, T_{db} is the dry bulb temperature $({}^{\circ}C)$, T_w is the temperature of water film $({}^{\circ}C)$, h_c is the convective heat transfer coefficient $(W\,m^2K^{-1})$, h_m is the mass transfer coefficient $(m\,s^{-1})$, h_{vs} is the latent heat of vaporization $(J\,kg^{-1})$, w_s is the saturated humidity ratio $(kg_w\,kg_a^{-1})$, and w_a is the humidity ratio $(kg_w\,kg_a^{-1})$. Considering that the rate of sensible heat removed from the air is equal to the latent heat gain rate from the evaporation of water we get,

$$h_c dA (T_a - T_w) = h_m h_{vs} dA (w_s - w_a)$$
 (10)

By assuming the inlet boundary conditions to be $T_{db} = T_{db,i}$ at x = 0, integrating eq.(9) we can obtain the change of temperature with thickness x as (Wu et al., 2009),

$$T_{db} = T_{wb} + \left(T_{db,i} - T_w\right) ex p\left(\frac{-h_c Ax}{\dot{m}_a C_{na}}\right)$$
 (11)

where T_{wb} is the wet-bulb temperature (°C), \dot{m}_a is the mass flow rate of air $(kg\ s^{-1})$, and C_{pa} is the specific heat of the air $(J\ kg^{-1}\ K^{-1})$. Through analysis of various numerical methods and empirical correlations of heat and mass transfer of DECs (He et al., 2015), we identified that the area of heat transferred used in the heat transfer equation of the cooling pad was the most significant one to predict the outlet conditions. Wu et al., (2009) presented the use of ξ , which is the pore surface coefficient per unit volume $(m^2\ m^{-3})$, which represents the total area that is in contact with the air. The ξ is specific for various cooling pad material and configuration (e.g., cellulose of 45°by 45° flutes with 147 sheets, $\xi = 345\ m^2\ m^{-3}$). This easily available ξ is the key to achieve model accuracy. Thus, the total area of heat transfer A is defined as,

$$A = \xi (b h d) \tag{12}$$

By assuming water film temperature T_w is approximately equal to T_{wb} and $\dot{m}_a = v_a \rho_a b h$, the cooling efficiency is derived by solving eq.(2) and eq.(11),

$$\eta = 1 - ex \, p \left(\frac{-h_c \, \xi \, d}{v_a \, \rho_a \, C_{pa}} \right). \tag{13}$$

The derived η is a function of h_c , d, v_a , C_{pa} and ξ . The h_c specific to the cooling pad can be determined by using the empirical correlations of Nusselt's number Nu, for convective heat transfer for flow across banks of tubed (Incropera et al., 1996), which is similar to that of the evaporative cooling pad media, with additional non-dimensional geometric parameter $\frac{l_e}{d}$,

$$Nu = C\left(\frac{l_e}{d}\right)^a Re^b Pr^{0.33},\tag{14}$$

where Nu is the Nusselt's number, Re is the Reynolds number, Pr is the Prandtl number, l_e is the characteristic length of the cooling pad (m), which is calculated by dividing the volume $V(m^3)$, of the cooling pad by the total wetted surface area A, and coefficients C, a, and b are determined based on experimental testing of the cooling pad. Re and Pr are determined by,

$$Re = \frac{\rho_a \, v_a \, d}{\mu_a},\tag{15}$$

$$Pr = \frac{c_{pa} \ \mu_a}{k_a},\tag{16}$$

$$Nu = \frac{h_c l_e}{k_a},\tag{17}$$

where, μ_a is the dynamic viscosity of air $(Pa\ s)$; ρ_a is the density of air $(kg\ m^3)$; k_a is the thermal conductivity of air $(W\ m^{-1}\ K^{-1})$. For our modeling, we have identified the Nu correlations for the commonly used cooling pad media described in Table 2.

Table 2 Nu correlations for different cooling pad media

Evaporative pad media	Reynolds number	Pore surface coefficient per unit volume (m²/m³)	Nusselt's number correlations	Reference	
Rigid cellulose (CELdek)	1841 <re<2829< td=""><td>400</td><td>$Nu = 0.10 \left(\frac{l_e}{d}\right)^{0.12} Re^{0.8} Pr^{0.33}$</td><td>(Dowdy & Karabash, 1987)</td></re<2829<>	400	$Nu = 0.10 \left(\frac{l_e}{d}\right)^{0.12} Re^{0.8} Pr^{0.33}$	(Dowdy & Karabash, 1987)	
Ceramic coated rigid cellulose (GLASdek)	1841 <re<2829< td=""><td>520</td><td>$Nu = 0.07 \left(\frac{l_e}{d}\right)^{0.12} Re^{0.8} Pr^{0.33}$</td><td>(Rawangkul et al., 2008)</td></re<2829<>	520	$Nu = 0.07 \left(\frac{l_e}{d}\right)^{0.12} Re^{0.8} Pr^{0.33}$	(Rawangkul et al., 2008)	

Coconut coir	883 <re<1308< th=""><th>209</th><th>$Nu = 0.53 \left(\frac{l_e}{d}\right)^{0.46} Re^{0.8} Pr^{0.33}$</th><th>(Liao et al., 1998)</th></re<1308<>	209	$Nu = 0.53 \left(\frac{l_e}{d}\right)^{0.46} Re^{0.8} Pr^{0.33}$	(Liao et al., 1998)
Aspen	937 <re< 1390<="" td=""><td>220</td><td>$Nu = 0.25 \left(\frac{l_e}{d}\right)^{0.12} Re^{0.8} Pr^{0.33}$</td><td>(Maurya et al., 2014)</td></re<>	220	$Nu = 0.25 \left(\frac{l_e}{d}\right)^{0.12} Re^{0.8} Pr^{0.33}$	(Maurya et al., 2014)

Using the calculated η from eq.(13), we can determine the $T_{db,ou}$, using eq.(2). The corresponding w_{ou} is determined based on the assumption $T_{wb,in} = T_{wb,ou}$, using the psychrometric calculations described in Appendix. The water consumed is calculated using eq.(4)-(7), similar to the lumped model. Finally, the sensible heat transfer Q_s and latent heat transfer Q_l are calculated using the determined outlet properties of the air,

$$Q_s = \dot{m}_a C_p \left(T_{dh,ou} - T_{dh,in} \right), \tag{18}$$

$$Q_l = \dot{m}_a h_{vs} (w_{ou} - w_{in}). (19)$$

Pressure drop introduced by the pad media is critically important as it can impact the mass flow rate of air through it, as well as the power consumed by the fan to cater to the pressure drop. A universal pressure drop expression specific to evaporative cooling pads proposed by Franco et al. (2014) is used to determine $\Delta p_i(Pa)$,

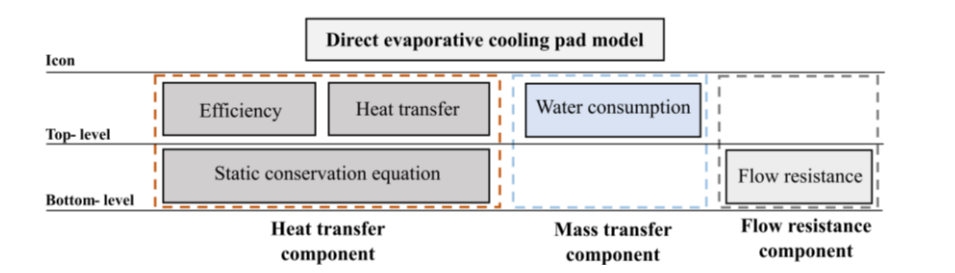
$$\Delta p_i = a \left(\frac{l_e}{d}\right)^b (1 + \dot{m}_w^c) v_a^2. \tag{20}$$

The Δp_i accounts for the impact of the mass flow rate of water \dot{m}_w , l_e , v_a . The coefficients a, b, and c can be calibrated for different cooling pads using values from the literature. The pump and fan models used in this work are from the Modelica buildings library and the underlying numerical equation used can be referred from Wetter (2013).

4. Model Implementation in Modelica

In this section, we first describe the Modelica implementation of the two variants of the cooling pad introduced in Section 3. Then we present the implementation of the DEC system model (Figure 1), using the developed cooling pad models and the existing fan and pump model from the Modelica buildings library (Wetter et al., 2014). Figure 3 shows the hierarchical structure of the DEC cooling pad model, which consists of three functions: heat transfer, mass transfer, and flow resistance. These functions are realized by using Modelica blocks which as commonly called components, implemented at different levels. Three top-level components include efficiency, heat transfer, and water consumption; and two bottom-level components include static conservation

equation and flow resistance. The combination of efficiency, heat transfer, and static conservation equation components realize the function of heat transfer. While the water consumption component with static conservation equation realizes the function of mass transfer. Finally, a flow resistance component with a fixed flow coefficient maintains the pressure drop. Both the variants of the cooling pad have the same internal hierarchical structure (Figure 4), yet the difference between the two cooling pad models is the underlying mathematical equation in the internal modules. This provides flexibility to interchange the variants for different modeling purposes. The pad models are built using the standard four-port interface of MBL with mixing volume and flow resistances connected on both the air and waterside. The ports are assigned with predefined media of MBL, the Buildings.Medium.Air and Buildings.Medium.Water. The mixing volume component represents the air and water flowing through the cooling pad, to which the heat and mass are exchanged. These mixing volumes have the static conservation equation for energy and mass balance implemented and hence can calculate the outlet conditions of the medium based on the values from the input connections. The mixing volume on the airside (volAir) has a moisture port to add the evaporated water mass flow rate \dot{m}_{evap} , to the medium. Conversely, the total mass flow rate of water \dot{m}_{tot} , required for the process of evaporative cooling is removed from the fluid port of the mixing volume on the waterside (volWat). The flow resistance creates a pressure drop between the inlet and outlet ports for different mass flow rates m, using the nominal pressure drop value Δp , either from calculations, catalog or from engineering standards.



Air side port al port bl outlet Outlet

Outlet

Water side

Water side

Figure 3 Hierarchical structure of the cooling pad model.

Figure 4 Icon of cooling pad model

4.1 Lumped Model for DEC Cooling Pad

Figure 5 represents the Modelica implementation for the lumped cooling pad model. The air/water inlet and outlet ports enable the connection of the cooling pad to a DEC system or an AHU. The three top-level functions in Figure 3 are implemented as Modelica components. These components

use the user input values for the geometric and thermal characteristics of the cooling pad to determine the outputs. In addition, there are sensors connected to the air and waterside to measure the inlet properties of the medium. The component EffLum calculates the η , using the inlet air velocity v_a and pad thickness d and outputs the value. The component HeaTraLum, uses the output of EffLum as its input and determines the outlet dry bulb temperature $T_{db,ou}$. The output is used by the component WatCon to computes \dot{m}_{evap} , which is added to the mixing volume on the airside (volAir) and \dot{m}_{tot} , that is removed from the mixing volume on the waterside (volWat). The nominal pressure drops across the cooling pad and pipe connecting the pump and the top of the cooling pad is also a user input (determined from manufacturers' catalogs).

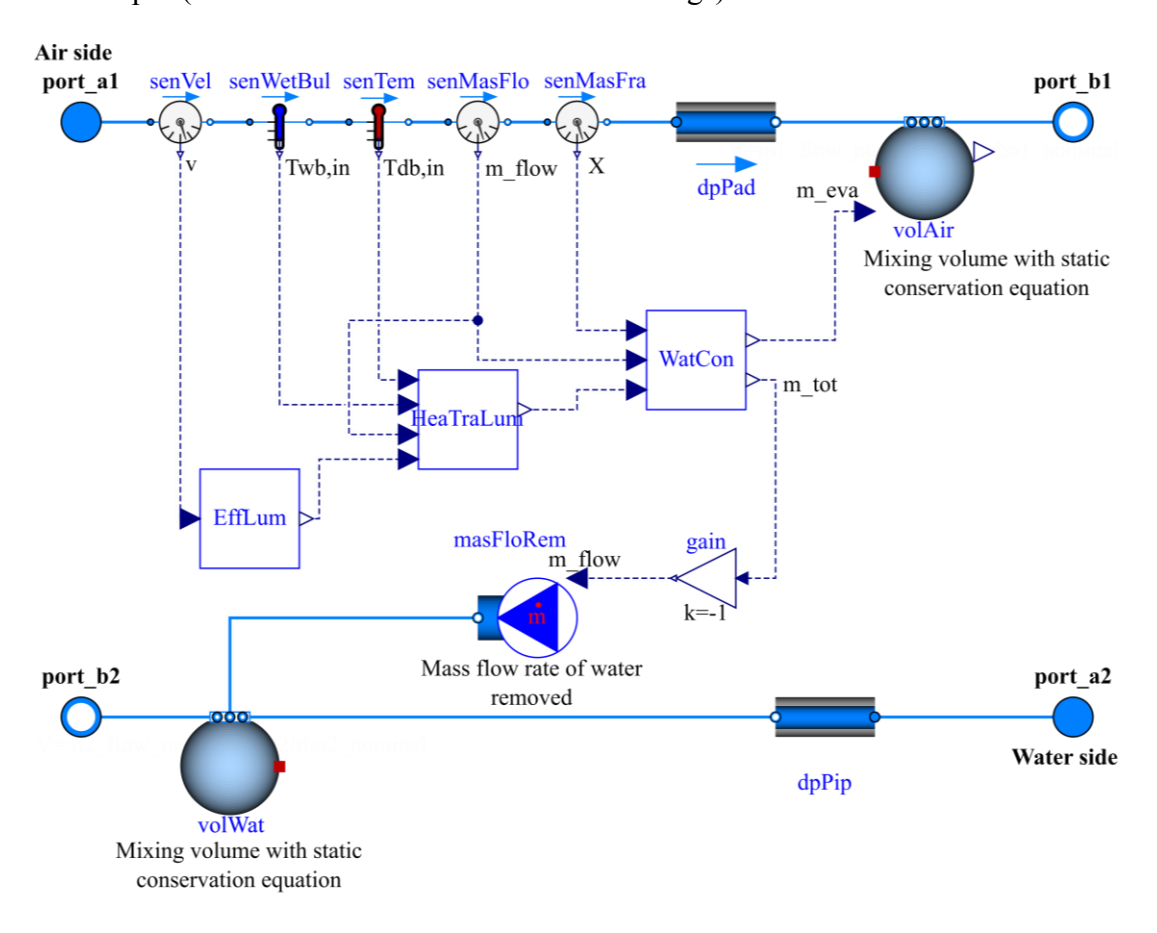


Figure 5 Modelica model of the lumped cooling pad

4.2 Physics-based Model for Cooling Pad

Figure 6, represents the Modelica implementation of the physics-based cooling pad. The hierarchical structure is similar to the lumped cooling pad model but differs in the detailed equations implemented (section 3.2). The block *Effphy* uses the geometric characteristics of the

cooling pad and the psychrometric properties of inlet air to calculate the heat transfer coefficient h_c , outlet dry bulb temperature $T_{db,ou}$ and outlet mass fraction w_{ou} . These outputs are used by both the HeaTraPhy and WatCon components. The HeaTraPhy, calculates and outputs the sensible and latent heat transfer, Q_s and Q_l . The component WatCon uses w_{in} , w_{out} and ρ_w to calculate the mass flow rate of water evaporated \dot{m}_{evap} , and the total mass flow rate of water consumed \dot{m}_{tot} , that is added to the air side (volAir) and removed from the water side (volWat) respectively. For the flow resistance function, the pressure drops Δp , across the cooling pad for the inlet mass flow rate \dot{m}_a is calculated using eq.(20) and is plugged into the dpPad. The waterside Δp_w is calculated based on the $\dot{m}_{w,nominal}$ and $\Delta p_{w,nominal}$ from the catalog specification of the DEC system in the dpPip.

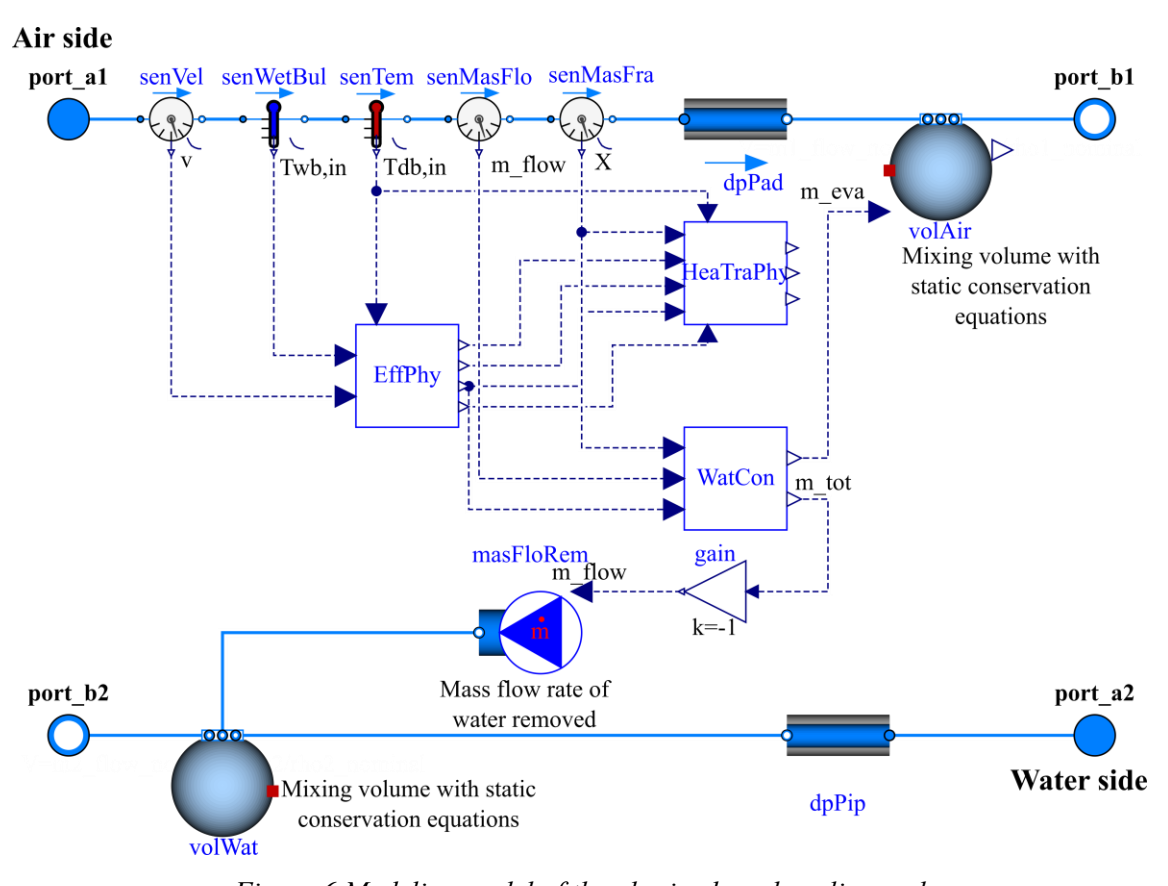


Figure 6 Modelica model of the physics-based cooling pad

4.3 Direct Evaporative Cooler Model

The DEC system model is implemented using the developed cooling pad models and the pump and fan component model from MBL. Figure 7 is the icon model of the DEC system and Figure 8

shows its internal components. The DEC system model is reduced to two ports representing only the airside, as the water is assumed to be recirculating within the reservoir. The cooling pad can be interchanged based on the modeling requirements. The fan model is implemented as an rpm input fan, as most commercially available DEC systems run on multiple speeds. The fan curves specific to the system evaluated can be used as the model input. The DECs typically have constant mass flow pumps; hence the pump model is implemented as mass flow input, requiring $\dot{m}_{w,nominal}$ and $\Delta p_{w,nominal}$ as inputs. This model outputs the total mass flow rate of water consumed as watCon; pump and fan power as pumP and fanP respectively.

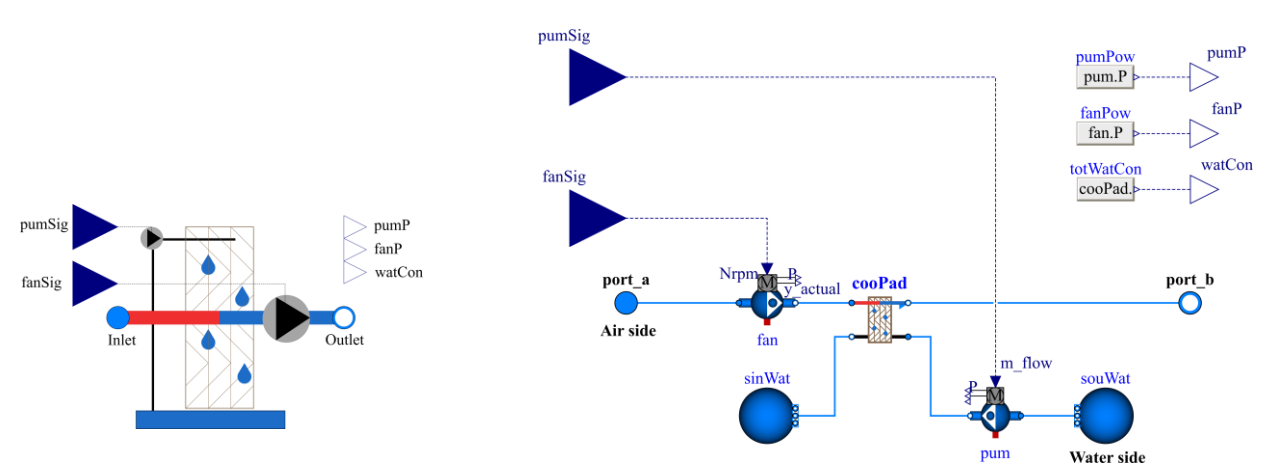


Figure 7 Modelica icon of the DEC Figure 8 Modelica model of the DEC system model with built-in system fan and pump

5. Model Validation

For validation, we implemented the DEC with a physics-based cooling pad connected to a source and a sink representing the boundary conditions of the inlet and outlet air (Figure 9). A duct resistance, dry bulb, and wet bulb sensors are added to the outlet of the DEC. Various experimental data from the literature are used for evaluating different parameters of the model represented in Table 3. The DEC with lumped cooling pad is also tested for comparison. As the lumped model is less sophisticated, it only calculates a few outputs, and thus has limited evaluation. The root mean squared error (RMSE) and normalized mean bias error (NMBE) metrics are used to evaluate the performance of the developed models. RMSE can indicate the model's ability to predict the overall load shape that is reflected in the data, and positive and negative values of NMBE can determine if the model over or underpredicts the data points.

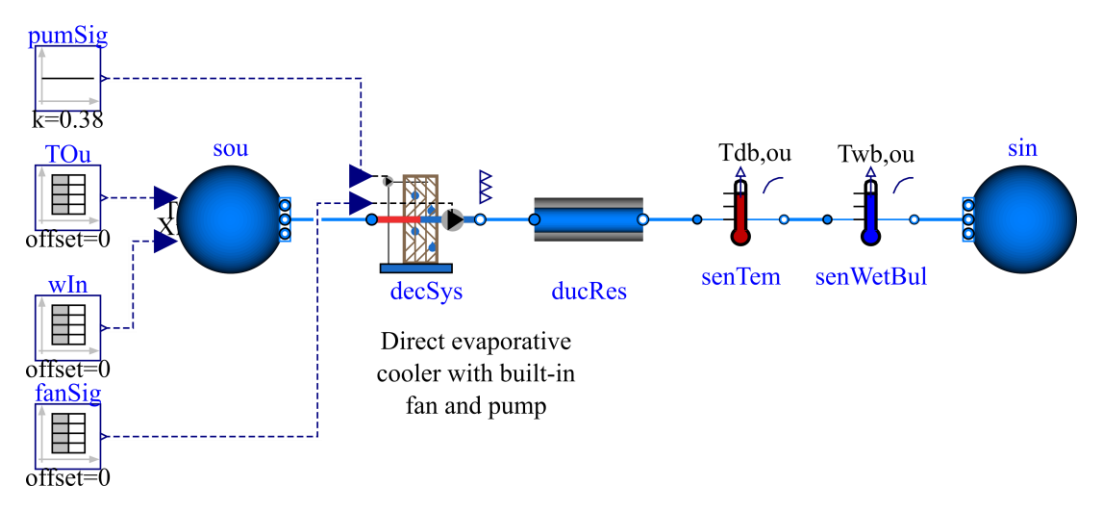


Figure 9 Modelica model of the DEC system with boundary conditions used for validation

Table 3 Model outputs used for comparing the performance.

Model outputs	Lumped	Physics-based	Reference results for comparison		
	model	model			
Efficiency, η	Yes	Yes	(Davis & Elberling, 2007)		
Pressure drops, Δp	No	Yes	(Franco et al. 2014)		
Power, P	Yes	Yes	(Davis & Elberling, 2007)		
Pad media	No	Yes	(Jain & Hindoliya, 2011; Rawangkul et		
			al., 2008; Maurya et al., 2014)		
Water consumption, \dot{m}_{tot}	Yes	Yes	(Davis & Elberling, 2007)		

5.1 Evaluation of the Efficiency Performance

The measured data from the performance test report of the Breezier evaporative cooler (Icon170) by PG&E is used for the validation (Davis & Elberling, 2007). This performance test follows the ASHRAE 133 standard for testing the DEC. The Modelica simulations are run with the same boundary conditions as that of the experiment ($T_{db,in}$,=31.8 - 42.8 °C, $T_{wb,in}$ = 18.8-19.5 °C, m_a = 0 -2.5 Kg/s, at 5 different rpm) with the catalog specifications of the Breezier DEC system (Icon 170) and CelDek cooling pad (Munters 440). The manufacturer's performance and system curves are used for calibrating the fan model (Seeley International, 2015). The outlet conditions

 $(T_{db,in},T_{wb,out})$ from the simulation results are used to calculate the efficiency η , using the relationship from eq.(2). The cooling efficiency of the DEC system for various mass flow rates is presented in Figure 10. The η of the physics-based model closely follows the experimental data, whereas the lumped model follows a similar trend with an offset. The clustered points in experimental data represent a slight change in η at each speed with varied inlet conditions, however, this is not distinctly reflected in the physics-based model. Figure 11 presents the η at varied inlet air dry bulb temperature and wet bulb depression ($WBD = T_{db} - T_{wb}$). The physics-based model closely overlaps the experimental η at WBD between 14-19 °C, exhibiting a minimum error for $T_{db,in}$ = 40.8 °C cases. From Table 4, the lumped model underpredicts the η by 11.5% with an RMSE=9.9, whereas the physics-based model overpredicts by 0.6% with an RMSE=1.2. As the lumped model follows the experimental data with a constant offset, if calibrated using a correction coefficient for the curve fit eq.(1), it can result in a lesser error. But obtaining a correction factor for each type of cooling pad can be difficult in practice. Hence, the physics-based model has the advantage compared to the lumped model due to its accurate prediction without any calibration of the cooling pad and system parameters.

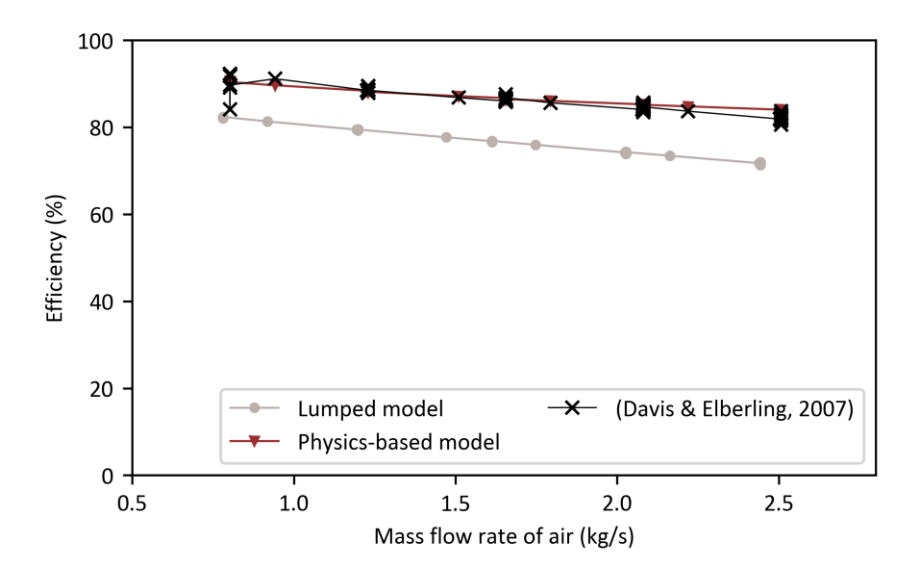


Figure 10 Efficiency of the cooling pad for various inlet mass flow rates of air.

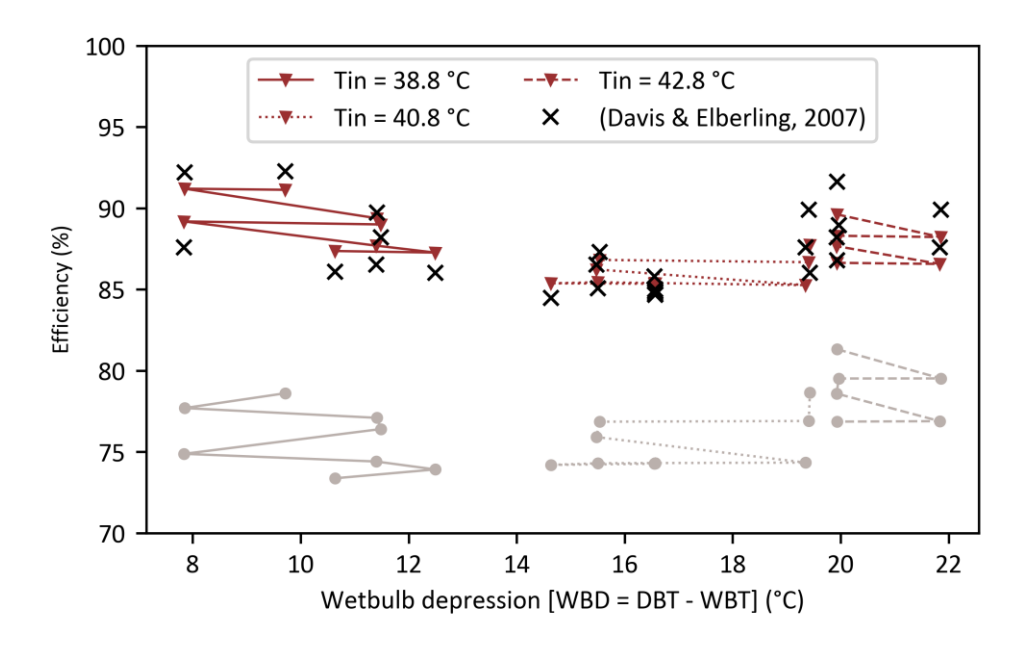


Figure 11 Efficiency of the cooling pad for various wet-bulb depressions.

5.2 Evaluation of Water Consumption

The volume of water consumption is an important aspect of assessing the performance of DEC; therefore, it is essential to have an accurate prediction. The lumped and the physics-based cooling pad models use the same equation for calculating the water consumption, yet the difference in \dot{m}_{tot} , occurs due to the variation in w_{ou} , which is a function of η . A similar trend as that of the efficiency performance can be observed for water consumption values represented in Figure 12. The vertical lines of data points represent the water consumption at each speed and the physics-based model closely follows the experimental water consumption data. While observing the water consumed at varied inlet air dry bulb temperature and wet bulb depression (Figure 13), there is a minimum error for WBD between 14-22 °C for $T_{db,in}$ =40.8 to 42.8 °C. From Table 4, the lumped model underpredicts the water consumed by 13.7% with an RMSE=0.001, whereas the physics-based model overpredicts by 0.9% with an RMSE=0.0004.

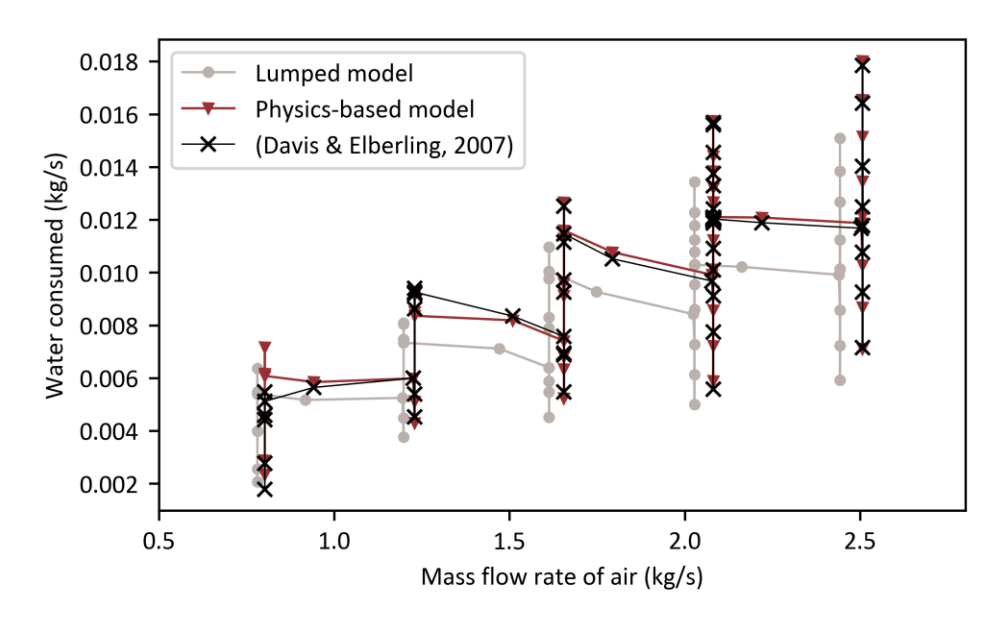


Figure 12 Water consumed for various inlet mass flow rates of air.

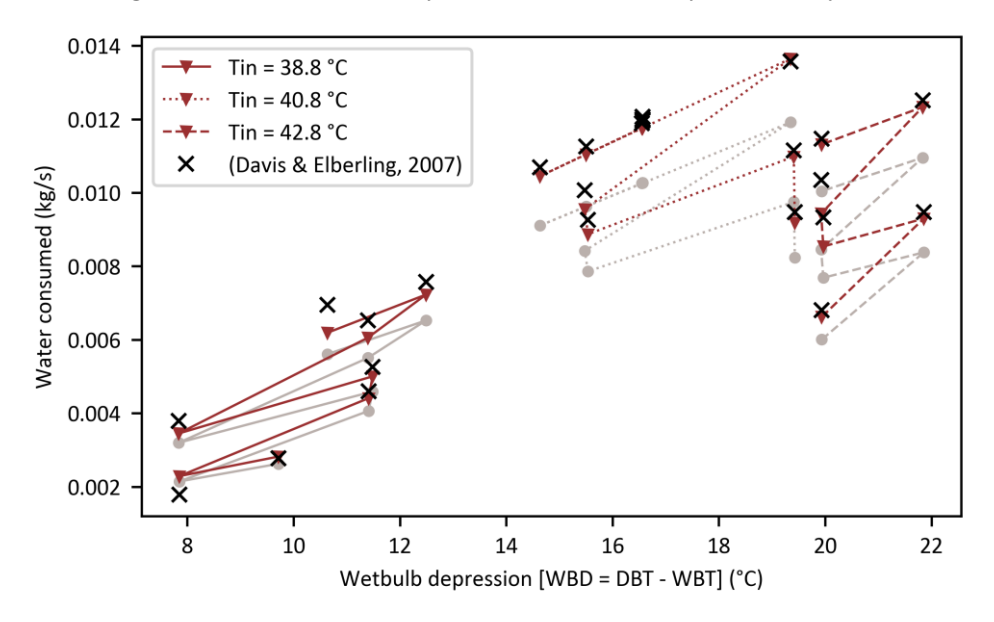


Figure 13 Water consumed for various wet-bulb depression and inlet dry bulb temperature.

5.3 Evaluation of Power Consumption

In Modelica models, the predicted power consumption of the fan is based on the pressure drop curve and the system curve used as input. To minimize errors, the system curves derived from the experimental result are used for calibration (Davis & Elberling, 2007), instead of the system design curves available from the catalog (Seeley International, 2015). Figure 14 presents the total energy consumed by both pump and the fan. The pumps consume a constant 30W throughout the operation and the variation in power is contributed by the fan. Both the lumped and physics-based cooling

pad models have a similar trend and closely followed the experimental data. The experiment data showed slight variations of the power consumption at a particular speed/rpm, which can be identified as the clustered data points; however, this is not observed in both lumped and the physics-based model. From Table 4, the lumped model underpredicts the power consumed by 11.7% with an RMSE=75.1, and the physics-based model underpredicts by 3.6 % with an RMSE=28.7. Although the lumped and physics-based models use the same fan models, the latter is more accurate due to the precise calculation of the pressure drop across the cooling pad, which impacts the fan power.

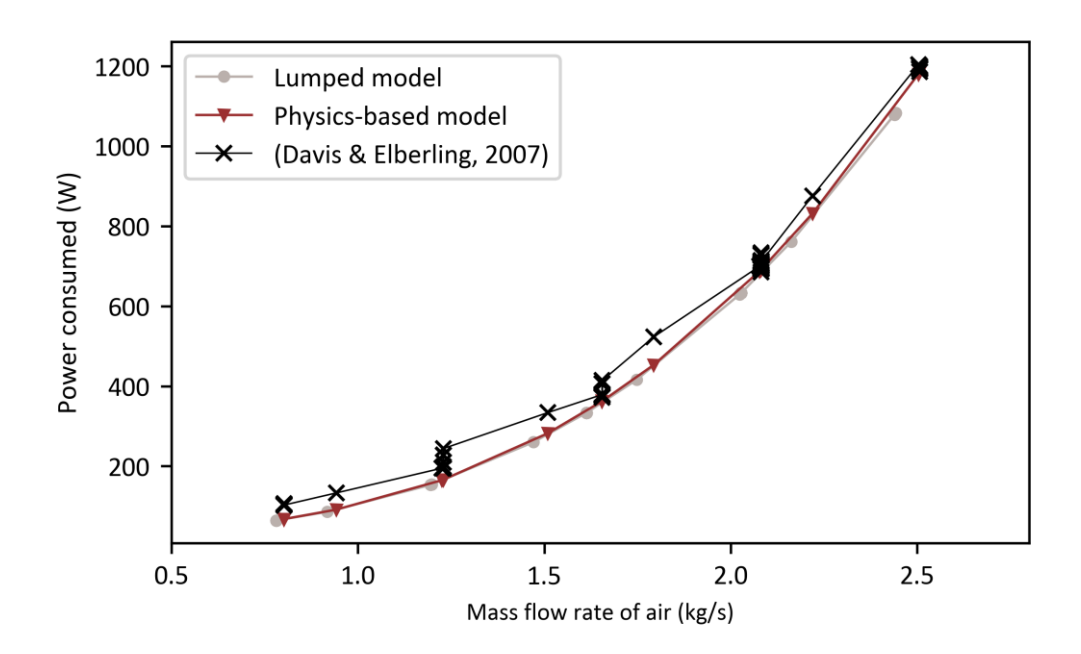


Figure 14 Power consumed at various mass flow rates of air

5.4 Evaluation of Pressure Drop

The experiment results from Franco et al. (2014) are used for validating the pressure drop equation implemented in the DEC model. The pressure drops values from the simulation, for two different pad thicknesses (d = 50mm and 100mm, cellulose pads with 45° by 45° flutes) under several inlet air velocities v_a , are compared with the experimental results. The coefficients of the generic pressure drop eq.(20) has been calibrated for this experimental case:

$$\Delta p_i = 0.786 \left(\frac{l_e}{d}\right)^{-0.469} (1 + m_w^{1.139}) v_a^2.$$
 (21)

Since the lumped cooling pad model uses a nominal pressure drop user input value for calculations, only the physics-based cooling pad model is considered for validation. The fan model is calibrated with the performance cur e s of HCT-45-2T-3/AL which is used in the experiment. From Figure 15, the pressure drop curve closely aligns with the experimental data for velocities less than 2.5m/s, whereas for higher velocities there is a larger error observed. From Table 4, the physics-based model underpredicts the pressure drop by 4.7% for a 50 mm thick cooling pad and 10.1% for a 100 mm thick cooling pad. Moreover, the velocity prediction of the model also is under-predicted between 2-6.8%. Although the accuracy of pressure drop prediction for thicker cooling pads reduces considerably, it is within \pm 10% acceptable limit. Thus, the model can compute the pressure drop for different thicknesses of the cooling pad without the need for nominal pressure drop values as input.

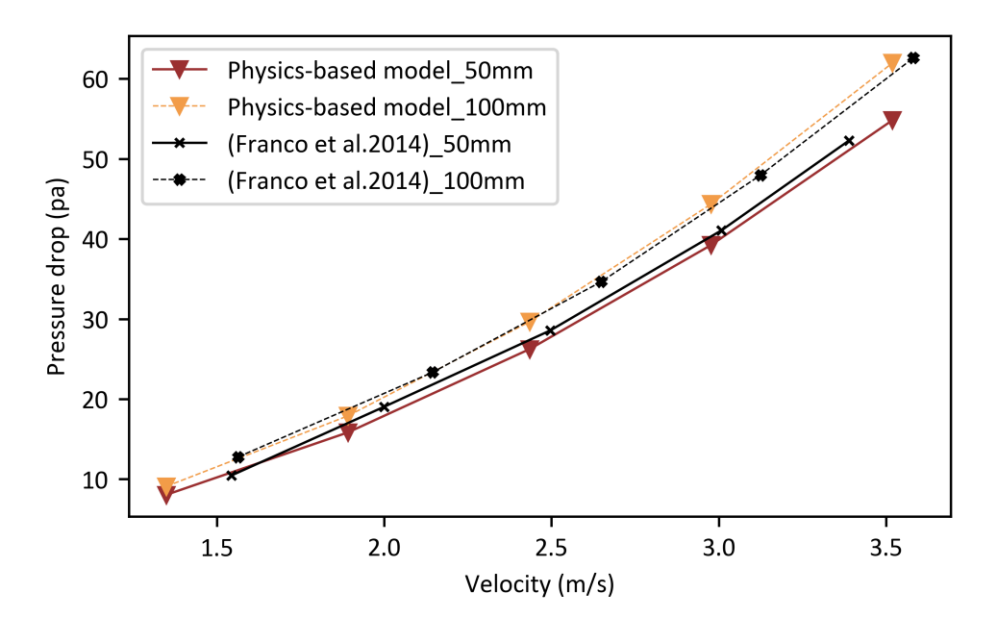


Figure 15 Pressure drops across the different thicknesses of the cooling pad (d=50mm, 100mm) and air velocity.

5.5 Evaluation with Different Pad Materials

Traditional evaporative cooling media is made of aspen or wooden cooling pads. With advancements in research and testing, the traditional media is replaced by engineered, plastic, or ceramic coated cellulose and rigid cellulose cooling pads. The model is simulated for four different pad media, varying in pore surface coefficient per unit volume ξ , and Nu correlation coefficients. Figure 16 presents the η simulated (S) and measured (M) for four different pad media for different

 v_a . The model can accurately predict the η of GLASdek and CELdek media with -0.37% and 1.8% errors, respectively. Whereas the error in predicting the η for aspen and coir media is 4.8% and -9.11% respectively. This difference in error percentages is due to the lack of availability of the ξ values for the coir and aspen pads. There pads are organically made, in contrast to the factory-made CELdek or GLASdek pads whose ξ are precisely determined. Calibrating the ξ of aspen and coir pads can result in reduced error.

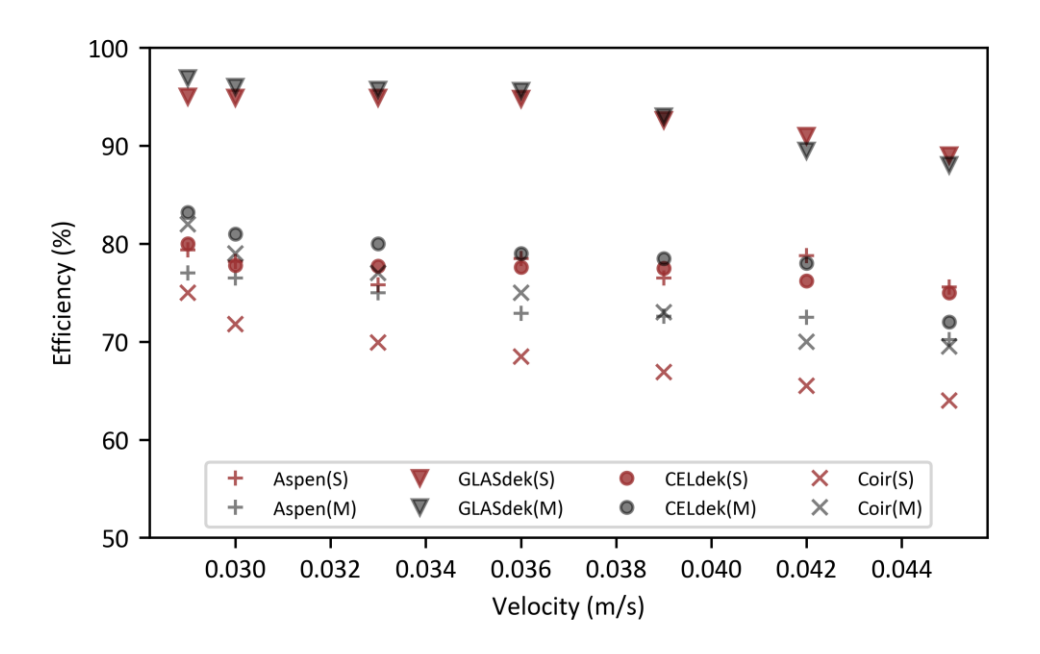


Figure 16 Saturation efficiency for different face velocities for various evaporative cooling media

Summarizing the results in Table 4, it is evident that the physics-based cooling pad model has an accurate prediction with NMBE between 0.6% to 3% for parameters related to heat and mass transfer, and NMBE between 2% to 10% for parameters related to the pressure drop. Whereas the lumped model has the NMBE in the range of 11-13%, with lesser outputs and hence cannot be used for detailed simulations. The physics-based model can predict the overall load shape that is reflected in the data based on the RMSE values. Apart from the lesser RMSE and NMBE, the physics-based cooling pad model is also found to be capable of simulating the performance of different evaporative cooling media. Currently, we have implemented the *Nu* correlations for four commonly used cooling pad media, which can be extended as required.

Table 4 Summary of errors

Parameters evaluated	Units	Lumped model		Physics-based model	
		RMSE	NMBE (%)	RMSE	NMBE (%)
Efficiency	%	9.9	11.5	1.2	-0.6
Water consumption	kg/s	0.001	13.7	0.0004	-0.9
Power consumption	W	75.1	11.7	28.7	3.6
Pressure drop	pa	-	-	3.2	4.7-10%
Velocity	m/s	-	-	0.011	2.1-6.8%
Various pad media (efficiency)	%	-	-	3.2	-1.7

6. Conclusion

In this paper, we systematically formulated, implemented, and validated a direct evaporative cooler model in Modelica, comprising two variants of evaporative cooling pads. (i) a physics-based model for the cooling pad that only needs the nominal catalog data to compute the heat and mass transfer with less than 1.9 % error (average NMBE). (ii) a simplified model of the cooling pad (i.e., the lumped model) from EnergyPlus exhibiting a 12.3% error (average NMBE) compared to the experimental data. Both the models require the dimensions of the cooling pad (L, B, H) and nominal pump and fan curves as inputs. The key difference in the accuracy is due to the use of pore coefficient area per unit volume ξ in the physics-based model, which accounts for the porosity and the area of heat and mass transfer A_s . On the other hand, the lumped model from EnergyPlus uses a multivariate curve fit equation specific to the cooling pad used, which is not easily available in manufacturers' catalogs.

Other advanced models discussed in the literature section require additional input parameters such as the temperature of water at the media interface, parameters specific to the configuration of the cooling pad, heat and mass transfer correlation coefficients, correlation coefficients for elevated water temperatures, etc. for accurate model prediction; and few of the inputs are determined via experiments. Therefore, considering the balance between the availability of inputs and model accuracy, the physics-based model developed in this paper is well capable of performing detailed energy simulation with the easily accessible catalog data. With the component-based Modelica implementation, the developed model can be re-used at various scales such as (1) DEC system-level simulations combined with a room thermal model; (2) Simulating the cooling pad as a pre-cooling component for a central cooling system; (3) Combining the cooling pad model with the indirect evaporative cooling component and Dx coil to test the performance of a hybrid cooling system; (4) Humidity based control of the cooling pad, etc.

This research can be further extended to develop a package of evaporative coolers (direct, indirect, hybrid) which can aid the design and development of low energy cooling systems, pre-cooling peak load savings, develop new evaporative media, and establish comfort and energy-efficiency control algorithms for hot and dry climate zones.

Model Availability

The DEC model along with the underlying components and base classes are freely available in our open-source GitHub location: https://github.com/sbslab/DirectEvaporativeCooler/tree/jbps. The model package also includes the example and validation cases discussed in this paper. Any future additions and revisions to the models can also be found in the same location.

Acknowledgement

The first author was initially funded by IUSSTF (Indo-US Science and Technology Forum) via the BHAVAN (Building Energy Efficiency Higher & Advanced Network) student internship program at the University of Colorado Boulder. This research was supported by the National Science Foundation under Awards No. IIS-1802017. BIGDATA: Collaborative Research: IA: Big Data Analytics for Optimized Planning of Smart, Sustainable, and Connected Communities. This work also emerged from the IBPSA Project 1, an international collaborative project conducted under the umbrella of the International Building Performance Simulation Association (IBPSA). Project 1 aims to develop and demonstrate a BIM/GIS and Modelica Framework for building and community energy system design and operation.

This work was also supported by the Department of Science and Technology (DST), Government of India, pro ide d under the "Dri i ng Efficient Low-energy-cooling Technologies: Assessment to Tech-transfer (DELTA-T)" grant to CE T Uni e rsity ha ing sanction order number TMD/CERI/BEE/2016/056(C) and TMD/CERI/BEE/2016/056(G).

Reference

- A. Franco, D. L. Valera, A. Madueño, A. Peña, Franco, A., Valera, D. L., Madueño, A., & Peña, A. (2010). Influence of water and air flow on the performance of cellulose evaporative cooling pads used in mediterranean greenhouses. *Transactions of the ASABE*, 53(2), 565–576.
- Amer, O., Boukhanouf, R., & Ibrahim, H. G. (2015). A Review of Evaporative Cooling Technologies. *International Journal of Environmental Science and Development*, 6(2), 111–117.
- ASHRAE. (2013). 2013 ASHRAE Handbook—Fundamentals (IP).
- Boukhanouf, R., Ibrahim, H. G., Alharbi, A., & Kanzari, M. (2014). Investigation of an Evaporative Cooler for Buildings in Hot and Dry Climates. *Journal of Clean Energy Technologies*, *2*(3), 221–225.
- Camargo, J., & Ebinuma, C. (2003). A Mathematical Model for Direct and Indirect Evaporative Cooling Air conditioning Systems. *Revista Da Engenharia Térmica*, *2*(2), 30–34.
- Chen, Y., Luo, Y., & Yang, H. (2014). Fresh Air Pre-cooling and Energy Recovery by Using Indirect Evaporative Cooling in Hot and Humid Region A Case Study in Hong Kong. *Energy Procedia*, *61*, 126–130.
- Crawley, D. B., Lawrie, L. K., Winkelmann, F. C., Buhl, W. F., Huang, Y. J., Pedersen, C. O., Strand, R. K., Liesen, R. J., Fisher, D. E., & Witte, M. J. (2001). EnergyPlus: Creating a New-generation Building Energy Simulation Program. *Energy and Buildings*, *33*(4), 319–331.
- Dai, Y. J., & Sumathy, K. (2002). Theoretical Study on a Cross-flow Direct Evaporative Cooler Using Honeycomb Paper as Packing Material. *Applied Thermal Engineering*, 22(13), 1417–1430.
- Davis, R. A., & Elberling, L. (2007). Laboratory Evaluation of the Breezair Icon Direct Evaporative Cooler. In *Pacific Gas and Electric Company*.
- Dodoo, A. (2011). Life Cycle Primary Energy Use and Carbon Emission of Residential Buildings. *Mid Sweden University*, *115*, 82.
- Dowdy, J. A., & Karabash, N. S. (1987). Experimental Determination of Heat and Mass Transfer Coefficients in Rigid Impregnated Cellulose Evaporative Media. *ASHRAE Transactions*, *93*(2), 382–395.

- Dowdy, J. A., Reid, R. L., & Handy, E. T. (1986). Experimental Determination of Heat-and Mass-transfer Coefficients in Aspen Pads. *ASHRAE Transactions*, *92*(2), 60–70.
- Elmqvist, H., & Mattsson, S. E. (1997). Modelica the Next Generation Modeling Language an International Design Effort. *Proceedings of the 1st World Congress on System Simulation*, 1–5.
- Fouda, A., & Melikyan, Z. (2011). A Simplified Model for Analysis of Heat and Mass Transfer in a Direct Evaporative Cooler. *Applied Thermal Engineering*, *31*(5), 932–936.
- Franco, A., Valera, D. L., & Peña, A. (2014). Energy Efficiency in Greenhouse Evaporative Cooling Techniques: Cooling Boxes Versus Cellulose Pads. *Energies*, 7(3), 1427–1447.
- Halasz, B. (1998). A General Mathematical Model of Evaporative Cooling Devices. *Revue Generale de Thermique*, 37(4), 245–255.
- He, S., Gurgenci, H., Guan, Z., Huang, X., & Lucas, M. (2015). A review of wetted media with potential application in the pre-cooling of natural draft dry cooling towers. *Renewable and Sustainable Energy Reviews*, 44, 407–422.
- Holman, J. P. (1988). Thermodynamics. McGraw-Hill, New York.
- IESVE. (2011). Version 6.2, Integrated Environmental Solutions Virtual Environment.
- Incropera, F. P., DeWitt, D. P., Bergman, T. L., & Lavine, A. S. (1996). Fundamentals of heat and mass transfer (Vol. 6). Wiley New York.
- Jaber, S., & Ajib, S. (2011). Evaporative Cooling as an Efficient System in Mediterranean Region. *Applied Thermal Engineering*, *31*(14–15), 2590–2596.
- Jain, J. K., & Hindoliya, D. A. (2011). Experimental Performance of New Evaporative Cooling Pad Materials. *Sustainable Cities and Society*, *1*(4), 252–256.
- Jorissen, F., Boydens, W., & Helsen, L. (2018). Validated Air Handling Unit Model Using Indirect Evaporative Cooling. *Journal of Building Performance Simulation*, 11(1), 48–64.
- Kachhwaha, S. S., & Prabhakar, S. (2010). Heat and Mass Transfer Study in a Direct Evaporative Cooler. *Journal of Scientific and Industrial Research*, 69(9), 705–710.
- Kettleborough, C. F., & Hsieh, C. S. (1983). The Thermal Performance of the Wet Surface Plastic Plate Heat Exchanger used as an Indirect Evaporative Cooler. *Journal of Heat Transfer*, 105(2), 366–373.
- Ko a če i ć, I., & ourbron, M. (207). The Numerical Model for Direct E aporati e Cooler. *Applied Thermal Engineering*, 113, 8–19.

- Kowalski, P., & Kwiecień, D. (2020). E a luation of imple E a porati e Cooling ystems in an Industrial Building in Poland. *Journal of Building Engineering*, *32*, 101555.
- Liao, C. M., Singh, S., & Wang, T. Sen. (1998). Characterizing the Performance of Alternative Evaporative Cooling Pad Media in Thermal Environmental Control Applications. *Journal of Environmental Science and Health*, *33*(7), 1391–1417.
- Maclaine-Cross, I. L., & Banks, P. J. (1981). A General Theory of Wet Surface Heat Exchangers and its Application to Regenerative Evaporative Cooling. *Journal of Heat Transfer*, 103(3), 579–585.
- Maurya, R., Shrivastava, N., & Shrivastava, V. (2014). Performance evaluation of alternative evaporative cooling media. *International Journal of Scientific & Engineering Research*, 5(10), 676–684.
- Mehrfeld, P., Lauster, M., Huchtemann, K., & Müller, D. (2016). Multi-mode Model of an Air Handling Unit for Thermal Demand Calculations in Modelica. *Building Simulation and Optimization, Third IBPSA England Conference*.
- Min, Y., Chen, Y., Shi, W., & Yang, H. (2021). Applicability of Indirect Evaporative Cooler for Energy Recovery in Hot and Humid Areas: Comparison with Heat Recovery Wheel. *Applied Energy*, 287, 116607.
- Plessis, G., Kaemmerlen, A., & Lindsay, A. (2014). BuildSysPro: a Modelica Library for Modelling Buildings and Energy Systems. *Proceedings of the 10th International Modelica Conference*, *96*, 1161–1169.
- Rawangkul, R., Khedari, J., Hirunlabh, J., & Zeghmati, B. (2008). Performance Analysis of a New Sustainable Evaporative Cooling Pad made from Coconut Coir. *International Journal of Sustainable Engineering*, *1*(2), 117–131.
- Sajjad, U., Abbas, N., Hamid, K., Abbas, S., Hussain, I., Ammar, S. M., Sultan, M., Ali, H. M., Hussain, M., Rehman, T. ur, & Wang, C. C. (2021). A Review of Recent Advances in Indirect Evaporative Cooling Technology. *International Communications in Heat and Mass Transfer*, 122, 105140.
- Saman, W., Bruno, F., & Tay, S. (2010). Technical Background Research on Evaporative Airconditioners and Feasibility of Rating their Energy Performance. In *Institute for sustainable systems and technologies*.
- Seeley International. (2015). The BreezairIcon Exq Series.

- Sodha, M. S., & Somwanshi, A. (2012). Variation of Water Temperature along the Direction of Flow: Effect on Performance of an Evaporative Cooler. *Journal of Fundamentals of Renewable Energy and Applications*, 2, 1–6.
- Trčka, M., Hensen, J. L. M., & Wetter, M. (2009). Co-simulation of Innovative Integrated HVAC Systems in Buildings. *Journal of Building Performance Simulation*, *2*(3), 209–230.
- Vakiloroaya, V., Samali, B., Fakhar, A., & Pishghadam, K. (2014). A Review of Different Strategies for HVAC Energy Saving. *Energy Conversion and Management*, 77, 738–754.
- Venkateswara Rao, V., & Datta, S. P. (2020). A Feasibility Assessment of Single to Multi/Hybrid Evaporative Coolers for Building Air-conditioning Across Diverse Climates in India. *Applied Thermal Engineering*, 168, 114813.
- Wetter, M. (2013). Fan and Pump Model that has a Unique Solution for any Pressure Boundary Condition and Control Signal. *Proceedings of 13th Conference of International Building Performance Simulation Association*, 3505–3512.
- Wetter, M., Zuo, W., Nouidui, T. S., & Pang, X. (2014). Modelica Buildings library. *Journal of Building Performance Simulation*, 7(4), 253–270.
- Weubbles, D. J. (1994). The Role of Refrigerants in Climate Change. *International Journal of Refrigeration*, 17(1), 7–17.
- Winkelmann, F. C., Birdsall, B. E., Buhl, W. F., Ellington, K. L., Erdem, A. E., Hirsch, J. J., & Gates, S. (1993). *DOE-2 Supplement: Version 2.1 E.* Lawrence Berkeley Lab,CA (United States).
- Wu, J. M., Huang, X., & Zhang, H. (2009). Numerical Investigation on the Heat and Mass Transfer in a Direct Evaporative Cooler. *Applied Thermal Engineering*, *29*(1), 195–201.

Appendix

This section describes the commonly used method for calculating the humidity ratio w, from dry $T_{db,in}$ and wet bulb temperature $T_{wb,in}$, of the process air (inlet). The w_{ou} of the air is calculated by assuming $T_{wb,in} = T_{wb,ou}$. The relative humidity of the outlet air φ , is calculated using:

$$e_d = 6.108 \exp\left(\frac{17.27 \ T_{db,in}}{237.3 + T_{db,ou}}\right),$$
 (22)

$$e_w = 6.108 \exp\left(\frac{17.27 \ T_{wb,ou}}{237.3 + T_{wb,ou}}\right),$$
 (23)

$$e = e_w - \left[0.00066 \left(1 + 0.00115 \, T_{ou,wb}\right) \left(T_{db,ou} - T_{wb,ou}\right) \left(\frac{p_{atm}}{100}\right)\right],\tag{24}$$

$$\varphi = \frac{\log\left(\frac{e}{6.108}\right),}{17.27}\tag{25}$$

where e_d is the saturation vapor pressure at dry bulb and e_w is the saturation vapor pressure at the wet bulb, e is the actual vapor pressure and p_{atm} is the atmospheric pressure. The dew point temperature T_{dew} is calculated by:

$$T_{dew} = \frac{237.3 \,\varphi}{1 - \varphi}.\tag{26}$$

The partial vapor pressure p_{wat} at T_{dew} is calculated as,

$$p_{wat} = 6.11 \exp\left(\frac{7.5 \, T_{dew}}{237.3 + T_{dew}}\right). \tag{27}$$

Using p_{wat} and p_{atm} , the w_{out} is calculated using:

$$X_{w} = 0.62198 \left(\frac{p_{wat}}{p_{atm} - p_{wat}} \right), \tag{28}$$

$$w_{out} = x_w \left(\frac{1}{1 + x_w}\right). \tag{29}$$